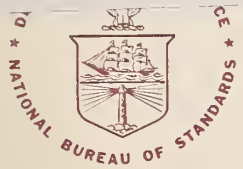

NBS TECHNICAL NOTE 1090

U.S. DEPARTMENT OF COMMERCE / National Bureau of Standards

Finline Diode Six-Port: Fundamentals and Design Information

M. Weidman

The National Bureau of Standards[1] was established by an act of Congress on March 3, 1901. The Bureau's overall goal is to strengthen and advance the nation's science and technology and facilitate their effective application for public benefit. To this end, the Bureau conducts research and provides: (1) a basis for the nation's physical measurement system, (2) scientific and technological services for industry and government, (3) a technical basis for equity in trade, and (4) technical services to promote public safety. The Bureau's technical work is performed by the National Measurement Laboratory, the National Engineering Laboratory, the Institute for Computer Sciences and Technology, and the Institute for Materials Science and Engineering.

The National Measurement Laboratory

Provides the national system of physical and chemical measurement; coordinates the system with measurement systems of other nations and furnishes essential services leading to accurate and uniform physical and chemical measurement throughout the Nation's scientific community, industry, and commerce; provides advisory and research services to other Government agencies; conducts physical and chemical research; develops, produces, and distributes Standard Reference Materials; and provides calibration services. The Laboratory consists of the following centers:

- Basic Standards[2]
- Radiation Research
- Chemical Physics
- Analytical Chemistry

The National Engineering Laboratory

Provides technology and technical services to the public and private sectors to address national needs and to solve national problems; conducts research in engineering and applied science in support of these efforts; builds and maintains competence in the necessary disciplines required to carry out this research and technical service; develops engineering data and measurement capabilities; provides engineering measurement traceability services; develops test methods and proposes engineering standards and code changes; develops and proposes new engineering practices; and develops and improves mechanisms to transfer results of its research to the ultimate user. The Laboratory consists of the following centers:

- Applied Mathematics
- Electronics and Electrical Engineering[2]
- Manufacturing Engineering
- Building Technology
- Fire Research
- Chemical Engineering[2]

The Institute for Computer Sciences and Technology

Conducts research and provides scientific and technical services to aid Federal agencies in the selection, acquisition, application, and use of computer technology to improve effectiveness and economy in Government operations in accordance with Public Law 89-306 (40 U.S.C. 759), relevant Executive Orders, and other directives; carries out this mission by managing the Federal Information Processing Standards Program, developing Federal ADP standards guidelines, and managing Federal participation in ADP voluntary standardization activities; provides scientific and technological advisory services and assistance to Federal agencies; and provides the technical foundation for computer-related policies of the Federal Government. The Institute consists of the following centers:

- Programming Science and Technology
- Computer Systems Engineering

The Institute for Materials Science and Engineering

Conducts research and provides measurements, data, standards, reference materials, quantitative understanding and other technical information fundamental to the processing, structure, properties and performance of materials; addresses the scientific basis for new advanced materials technologies; plans research around cross-country scientific themes such as nondestructive evaluation and phase diagram development; oversees Bureau-wide technical programs in nuclear reactor radiation research and nondestructive evaluation; and broadly disseminates generic technical information resulting from its programs. The Institute consists of the following Divisions:

- Inorganic Materials
- Fracture and Deformation[3]
- Polymers
- Metallurgy
- Reactor Radiation

[1] Headquarters and Laboratories at Gaithersburg, MD, unless otherwise noted; mailing address Gaithersburg, MD 20899.
[2] Some divisions within the center are located at Boulder, CO 80303.
[3] Located at Boulder, CO, with some elements at Gaithersburg, MD.

Finline Diode Six-Port: Fundamentals and Design Information

M. Weidman

Electromagnetic Fields Division
Center for Electronics and Electrical Engineering
National Engineering Laboratory
National Bureau of Standards
Boulder, Colorado 80303

U.S. DEPARTMENT OF COMMERCE, Malcolm Baldrige, Secretary

NATIONAL BUREAU OF STANDARDS, Ernest Ambler, Director

Issued December 1985

National Bureau of Standards Technical Note 1090
Natl. Bur. Stand. (U.S.), Tech Note 1090, 40 pages (Dec. 1985)
CODEN: NBTNAE

U.S. GOVERNMENT PRINTING OFFICE
WASHINGTON: 1985

For sale by the Superintendent of Documents, U.S. Government Printing Office, Washington, DC 20402

CONTENTS

		Page
1.	Introduction	1
2.	Preliminary design	2
	2.1 Materials and fabrication techniques	2
	2.2 Six-port geometries	2
	2.3 Transmission line type	5
3.	Initial hardware and testing	6
	3.1 Waveguide-finline-waveguide (WFW) transition	6
	3.2 Beam lead diode sensitivity and linearity tests	9
	3.3 Series slot tests	14
4.	Redesign	15
	4.1 Leakage correction	15
	4.2 Waveguide housing	16
	4.3 Taper design	17
	4.3.1 Dielectric taper	17
	4.3.2 Finline taper design	24
	4.3.3 Soft substrate designs	29
5.	Summary and future work	32
6.	Acknowledgment	32
7.	References	32

Finline Diode Six-Port: Fundamentals and Design Information

M. Weidman

Electromagnetic Fields Division
National Bureau of Standards
Boulder CO 80303

The preliminary design and testing of a planar circuit six-port with diode detectors is described. The planar circuit medium was chosen to be finline, and all preliminary work was done in WR-42 waveguide (18-26.5 GHz). The finline substrate was alumina, and initially commercial beam-lead diodes were bonded to the finline metalization. The goal is to design an integrated circuit which could be fabricated on one chip (with diode detectors) and used as part of a six-port network analyzer in the waveguide bands above 18 GHz. Initial designs proved to be unsatisfactory because of high losses and reflections. Most of the problems have been solved, and a usable integrated finline circuit is a good possibility for a millimeter wave six-port.

Key words: diode six-port; finline; integrated circuit; millimeter wave; network analyzer; planar circuit; six-port.

1. Introduction

A six-port is a linear passive network having six ports. It is used to measure the complex scattering parameters of devices from submicrowave to optical frequencies. One of the ports is connected to a signal source, another to the device under test, and the remaining four ports to power detectors. Present six-port work in the millimeter wave region has shown a need for sensitive detectors and smaller size six-port networks. Broadband power sources above 40 GHz have very limited (1 mW to 50 mW) power outputs. Thermistor power detectors on a dual six-port system would have less than tenths of milliwatts to work with, and this seriously degrades the performance of the system. Diode detectors would reduce source power requirements by 10-15 dB but would require additional calibration steps to characterize their nonlinear power response. The size of the six-port network plus detectors is critical because of the need for temperature control and problems with flange alignment and repeatibility. Temperature control is accomplished by housing the network and detectors in a proportionally controlled heat sink. A physically large

six-port, with the heat sink, is heavy and creates problems with flange alignment. An integrated diode finline six-port would be at least an order of magnitude smaller than existing designs.

Some of the early designs with finline on alumina pointed out loss and reflection problems. Most of these problems have now been solved, and the next step is to build a prototype six-port using beam-lead diodes bonded to the finline.

2. Preliminary design

2.1 Materials and fabrication techniques

It was decided that if the final design were to have diodes integrated into the microwave-millimeter wave circuit, a hard substrate such as alumina (Al_2O_3) should be used for preliminary microwave design and testing. NBS fabrication facilities were used as much as possible during the development stages. Metalization of the alumina was a thin layer of chrome (0.05 μm) and then gold built up to several skin depths (0.15 μm evaporated plus 3 μm plated). Quartz or glass could also be used as a substrate, but the initial idea was to eventually use silicon on sapphire technology, and alumina was chosen because of its similarity to sapphire.

2.2 Six-port geometries

Two types of six-port geometry were considered (fig. 1). The first uses three nondirectional probes along with one directional coupler to make a six-port network. The spacing of the three nondirectional probes should be approximately $\lambda_g/6$ where λ_g is the guide wavelength [1]. The second geometry can be realized by placing short circuits on the side arm of three directional couplers where there would normally be a matched termination [1]. The proper phase relationships between the detectors at the other side arm ports are obtained by making the relative distances to the three short circuits differ by $\lambda_g/6$. A series slot six-port is equivalent to the one using three nondirectional probes. The diodes are placed in series with the finline and spaced $\lambda_g/6$ apart. Figure 2 shows the two types of six-ports realized in finline. The series slot configuration has already been proven useful in a WR-42 waveguide six-port.

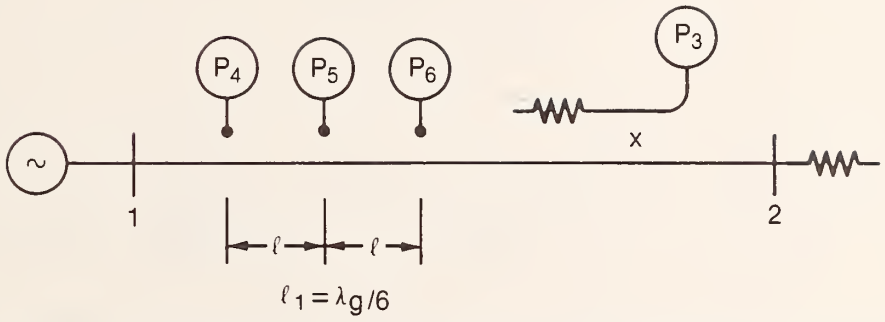

(a) Three nondirectional probes plus one directional coupler.

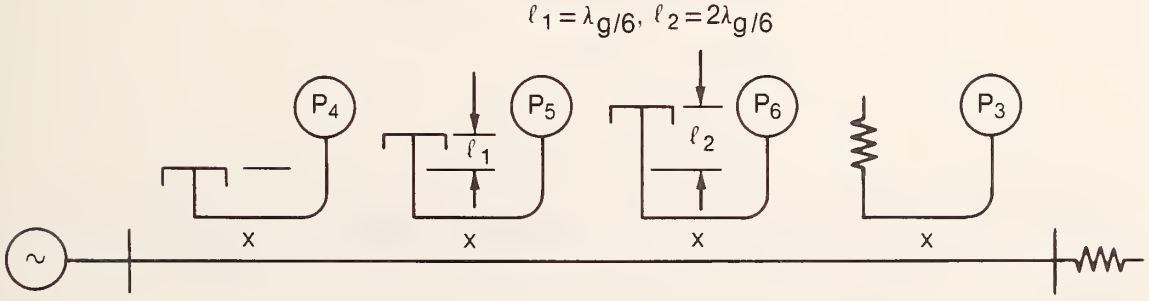

(b) Equivalent to (a) with shorted couplers.

Figure 1. Two convenient six-port realizations.

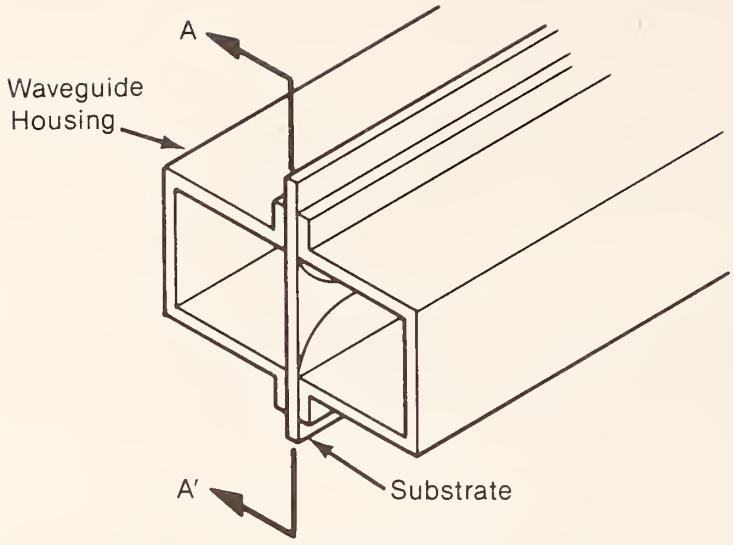

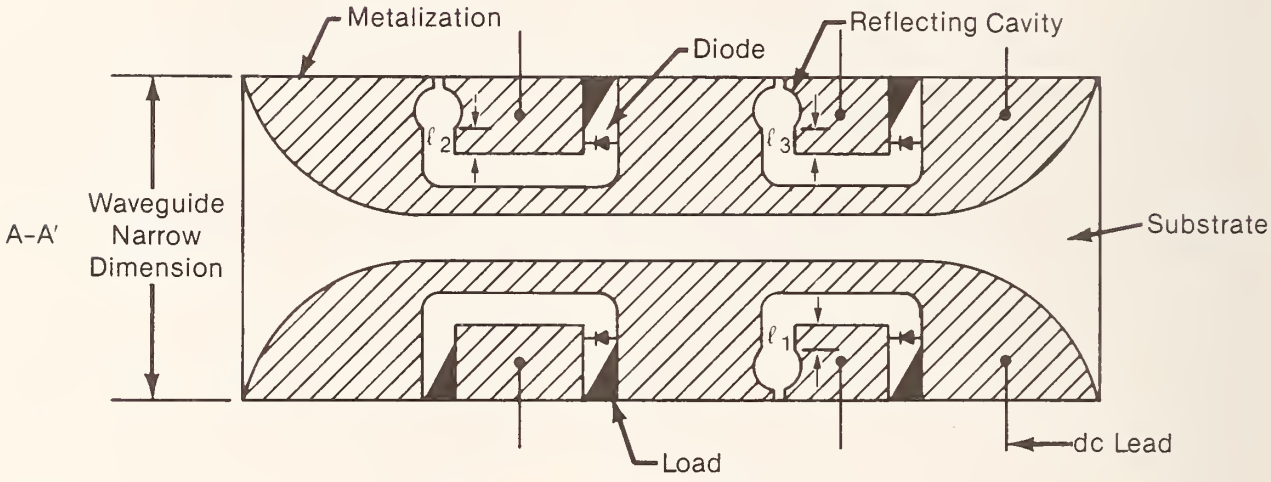

(a) Shorted coupler six-port

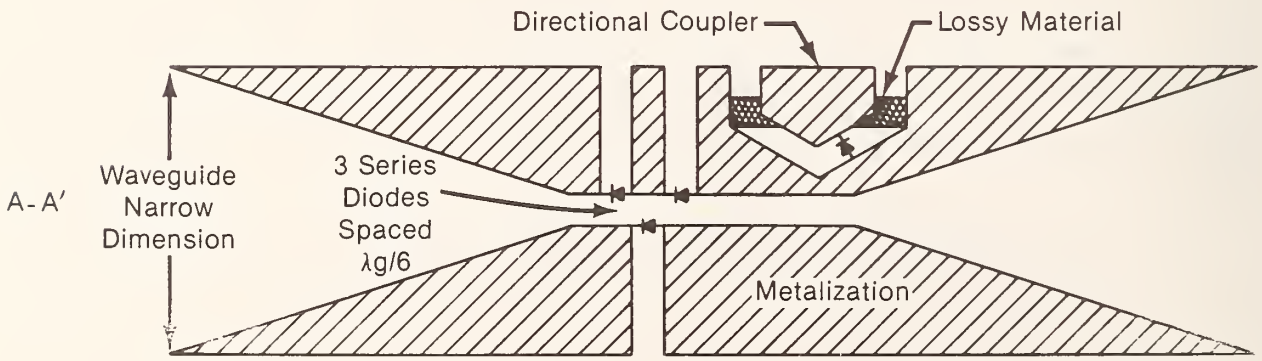

(b) Series slot six-port

Figure 2. Finline substrate metalization for two six-port geometries.

2.3 Transmission line type

After doing an extensive literature search, it was decided that finline would lend itself to the realization of a six-port with diode detectors. Finline, proposed by Meier [2], is a printed or metalized substrate circuit placed in rectangular waveguide in the E plane, or parallel to the electric field. In its simplest form it is a dielectric loaded, ridged waveguide with very thin ridges. Finline was chosen for its adaptability to rectangular waveguide and the integration of the diode detectors. The six-ports will be used mainly for rectangular waveguide measurements above 18 GHz. Two other types of transmission line which were considered for an integrated six-port are microstrip and suspended substrate, but they are not as easily adapted to waveguide as finline. Reference [3], with 94 references, gives a good summary of E plane millimeter wave technology.

After the decision to use finline, some initial design parameters were estimated using the available literature [4,5]. It was decided to do all the preliminary work in the WR-42 waveguide band (18-26.5 GHz). This is the lowest frequency band in the range of interest, and an existing single six-port could be used to make measurements on preliminary hardware. The main parameters of interest for designing the six-port in finline are λ_g (guide wavelength) and impedance. Impedance in finline or rectangular waveguide can be defined in more than one way, so care must be taken to understand which definition is used in the literature. Generally impedance can be defined as wave, voltage/current, $(\text{voltage})^2/\text{power}$, or $\text{power}/(\text{current})^2$.

The parameters λ_g and Z (impedance) are a function of waveguide dimensions (a and b), substrate thickness (s), substrate dielectric constant (ε_R), and slot width (d), all shown in figure 3. For alumina, ε_R is approximately 10. The thinnest practical substrate is about 0.1 mm, and if the design is to be scaled over the frequency range from 18 to 100 GHz, the substrate for WR-42 would be about 0.6 mm thick. The guide wavelength in a typical finline on 0.6 mm alumina substrate is approximately one half the free space wavelength (λ_0). A typical range of impedances is 100-400 ohms, depending on slot width (d) and impedance definition. From these initial rough estimates, some preliminary hardware was built and tested.

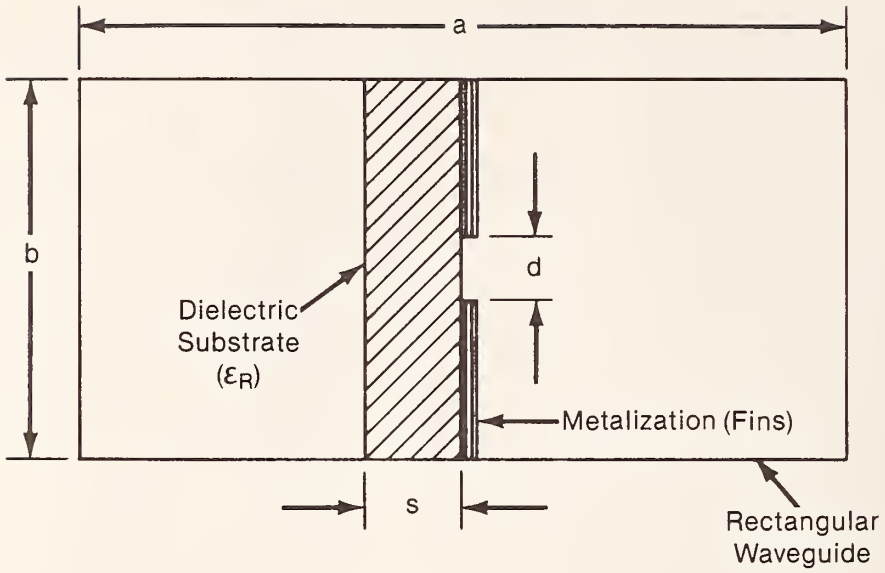

Figure 3. Unilateral finline cross section with relevant dimensions.

During the literature search on finlines, several papers were found on the design of finline and slotline directional couplers [6-12]. Finline is a special case of slotline, and for narrow gaps there is little difference between the two. Most of the finline papers give theory and data based on finlines built with soft duroid (ε_R = 2.22) substrates. The results from the literature were modified to approximate parameters for alumina substrate. An initial design for a finline directional coupler has been completed, but no fabrication or testing has been done to date.

3. Initial hardware and testing

3.1 Waveguide-finline-waveguide (WFW) transition

Since the six-port will be used to make measurements in rectangular waveguide, a transition to finline is necessary. Also, the only way to use the existing six-port to make finline measurements is at a rectangular waveguide port. Two transitions were fabricated on one 5 cm x 5 cm substrate. Figure 4 shows the two circuits. One finline has a center gap of 0.381 mm and the other 0.762 mm. The taper from the narrow waveguide dimension (4.318 mm) to the final finline gap is linear and approximately 20 mm long. The metalized substrate was placed through two 0.7 mm wide, longitudinal slots milled into the center of the broad walls of a WR-42 straight section of waveguide. The

metalized side was prevented from touching the waveguide by a thin (0.08 mm) sheet of Mylar. This was done so that all metalized sections are dc isolated. After centering the circuit in the waveguide, the narrow walls were squeezed with clamps to hold the substrate in place.

Initial loss and reflection tests showed much higher loss and reflection than anticipated (3-10 dB loss and reflection coefficient > 0.4). It appeared that there was considerable leakage from the finline where it protruded from the waveguide.

Initial loss measurements were made by placing a thermistor mount at the input and output of the transition and calculating P_{out}/P_{in}. Reflection coefficient measurements were made using the single six-port looking into one port of the transition with the other port terminated in a matched load. More accurate but time consuming sliding short loss measurements [13],

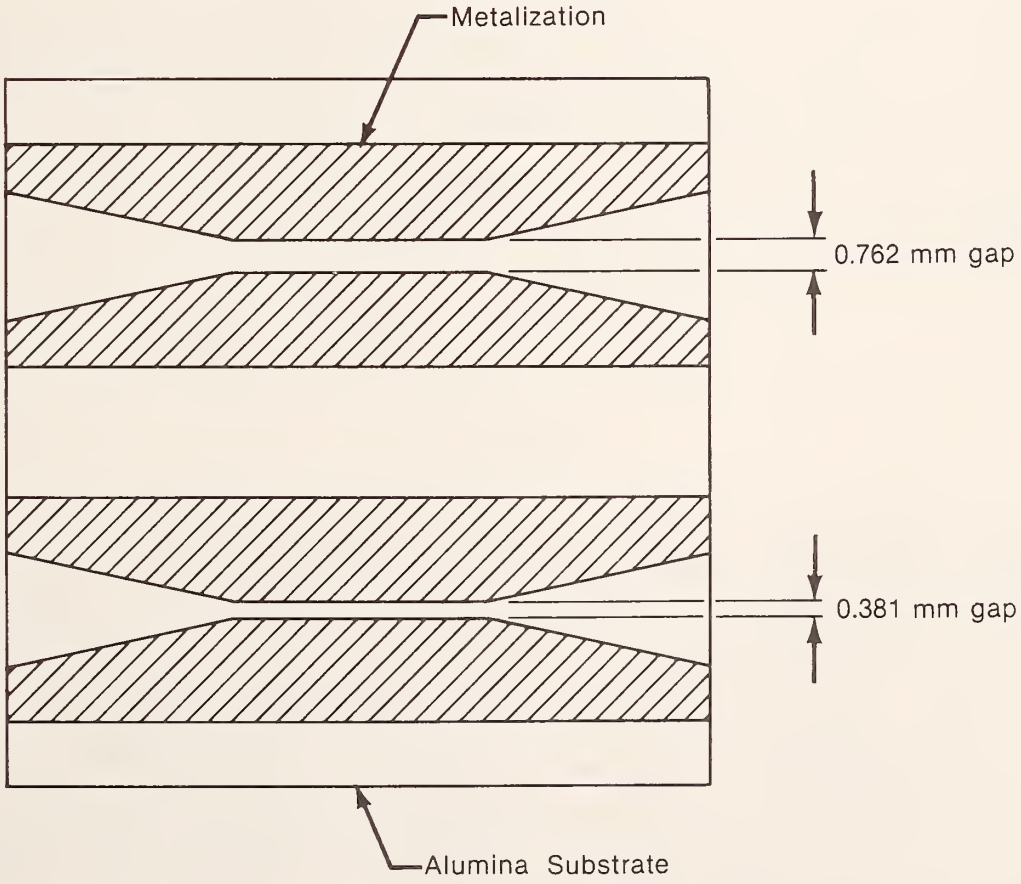

Figure 4. First finline fabrication (two waveguide-finline-waveguide transitions).

showed the loss of the waveguide-finline-waveguide transition (WFW) to be in the range of 3-5 dB for the 0.762 mm finline and 6-10 dB for the 0.381 mm finline.

The loss in dB measured with a sliding short is 10 log η_a, where η_a (two-port maximum efficiency) is

$$\eta_a = \frac{2T}{1 + \sqrt{1 - 4T^2}} \tag{1}$$

and

$$T = \frac{r}{1 + r^2 - r_c^2}, \tag{2}$$

$$r = \frac{|\Gamma|_{max} + |\Gamma|_{min}}{2}, \tag{3}$$

and

$$r_c = \frac{|\Gamma|_{max} - |\Gamma|_{min}}{2}. \tag{4}$$

The quantities $|\Gamma|_{max}$ and $|\Gamma|_{min}$ are the maximum and minimum reflection coefficients as measured by the six-port at the input to the WFW transition with a sliding short moved at the output.

Other loss parameters such as $|S_{21}|^2$ and $\eta_{a\ell}|_{\Gamma_\ell = 0}$ (efficiency of two-port with matched load) are

$$|S_{21}|^2 = r(1 - |S_{11}|)^2, \tag{5}$$

and

$$\eta_{a\ell}|_{\Gamma_\ell = 0} = r. \tag{6}$$

The loss varied considerably depending on finline orientation and clamping pressure. Additional plating was done on the metalization to assure enough skin depths of conductor, but the lowest loss achieved on the 0.762 mm finline was still in the 2-3 dB range. Later it was discovered that the metalization should extend only to the outside of the broad waveguide wall and not beyond it. Waves propagating at right angles to the normal transmission line mode will then see an open circuit $\lambda_d/4$ from the inside of the waveguide wall--λ_d is wavelength in the dielectric ($\varepsilon_R \approx 10$), and the standard waveguide wall thickness is approximately $\lambda_d/4$ (1 mm).

The reflection coefficient looking into the transition was in the range 0.1-0.5 across the band. Both loss and reflection were an order of magnitude worse than expected.

At this time tests were also made with a thin, lossy material placed so as to terminate the finline in the center of the finline section. This type of material would be used to terminate the side arm of a directional coupler or a broadband diode detector mount fabricated in finline. The lossy material was placed on either side of the substrate in the form of a tapered wedge between the two metalized fins. Location of the lossy material did not seem to affect the loss very much. The loss in this case was not nearly high enough. The terminated finline should have had a very high loss (> 40 dB). The primary loss and termination problems appeared to be caused by leakage out of the structure and leakage around the termination. The high reflection coefficient was caused mainly by the abrupt change from air filled waveguide to slab loaded waveguide.

3.2 Beam lead diode sensitivity and linearity tests

After completing the transition loss and reflection tests, a beam lead diode was attached across the 0.762 mm gap finline (using an ultrasonic bonder). One of the original ideas was to compare the reflection coefficient of the plain finline transition to the diode loaded finline. This would give some idea of the impedance relations between the finline and the diode. However, since the finline reflection was initially so high, no usable impedance information was obtained for the diode mounted in the finline.

Sensitivity and power linearity of the diode mounted in the finline structure were measured. The transition, with diode in place, was terminated by an adjustable short circuit at one of the ports. The other port was then the input of a tunable diode detector mount. Both direct dc detection (using a digital nanovoltmeter) and ac (source amplitude modulation with synchronous receiver at diode) were used. During these tests it was noted that since the diode was a low to medium barrier Schottky diode, dc bias (approximately 3 μA) had to be applied to the diode to achieve the lowest noise level. Sensitivity was determined by setting up a known amount of input power with a calibrated thermistor mount and then using a combination of level set and rotary vane

attenuators to reduce this power from +10 dBm to -60 dBm. The sliding short tuner on the output of the finline detector was adjusted to give maximum sensitivity at each frequency.

The noise level was near the predicted -50 dBm level. The actual specifications for Schottky diodes are in terms of TSS (tangential sensitivity) which is approximately 4 dB above the noise level. This compares to a bolometric detector (thermistor mount), more commonly used with six-port systems, of about -45 dBm using the best instrumentation (1 μV resolution voltmeter and low thermal relay scanner). Signal levels at the six-port detectors should be 40 dB above this noise level for 0.01 percent power resolution in order to fully utilize the six-port capability for measuring reflection coefficient. Improved diode and mounting design can probably improve the diode detector performance, at best, another 10 dB for an improvement of 15 dB over the thermistor detector. This means 15 dB less power required from the source. Sources in the range of 10-50 mW would be satisfactory.

Power linearity, or diode square law response, was measured using the same techniques described above. The linearity was compared with the rotary vane attenuator, which is accurate to within 0.02 dB in the lower portion of its range. The diode must be loaded (resistor in parallel with diode outside of waveguide) in order to even approach a square law response. The results of these measurements are shown in figures 5-7. Figure 5 shows the diode response with a 200 kΩ load resistor over a range of input power levels from 0 dBm to -50 dBm. The straight line is a perfect square law response. Figure 6 shows diode response for different values of load resistor. Figure 7 is an expanded vertical scale plot with both 100 kΩ and 200 kΩ load resistors. In the region of power levels in figure 7 (-48 dBm to -20 dBm), the diode detector should exhibit much better linearity. Perfect square law response would be a straight horizontal line. Any deviation from a straight line (>0.01 percent) adds an additional step to the six-port calibration. As can be seen from figure 7, there is an overall vertical spread of approximately 8.3 percent for the 100 kΩ load and 11.3 percent for the 200 kΩ load. This nonlinearity does not prohibit the use of the diode detector in a six-port system; but the smaller the correction the better. More work will be needed in the area of detector design (diode parameters and mounting in finline).

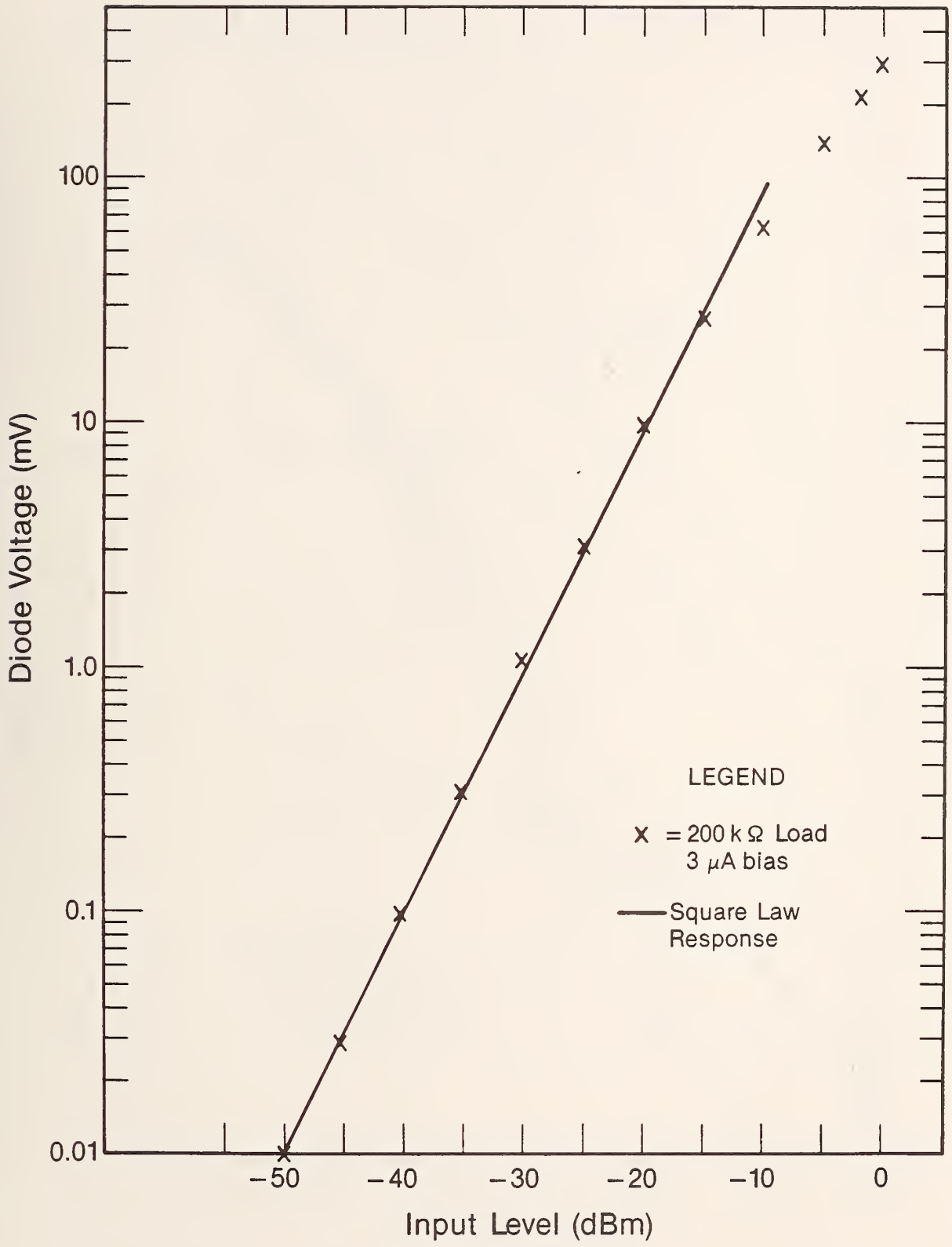

Figure 5. Finline diode detector response over the power range 0 dBm to −50 dBm (200 k Ω load).

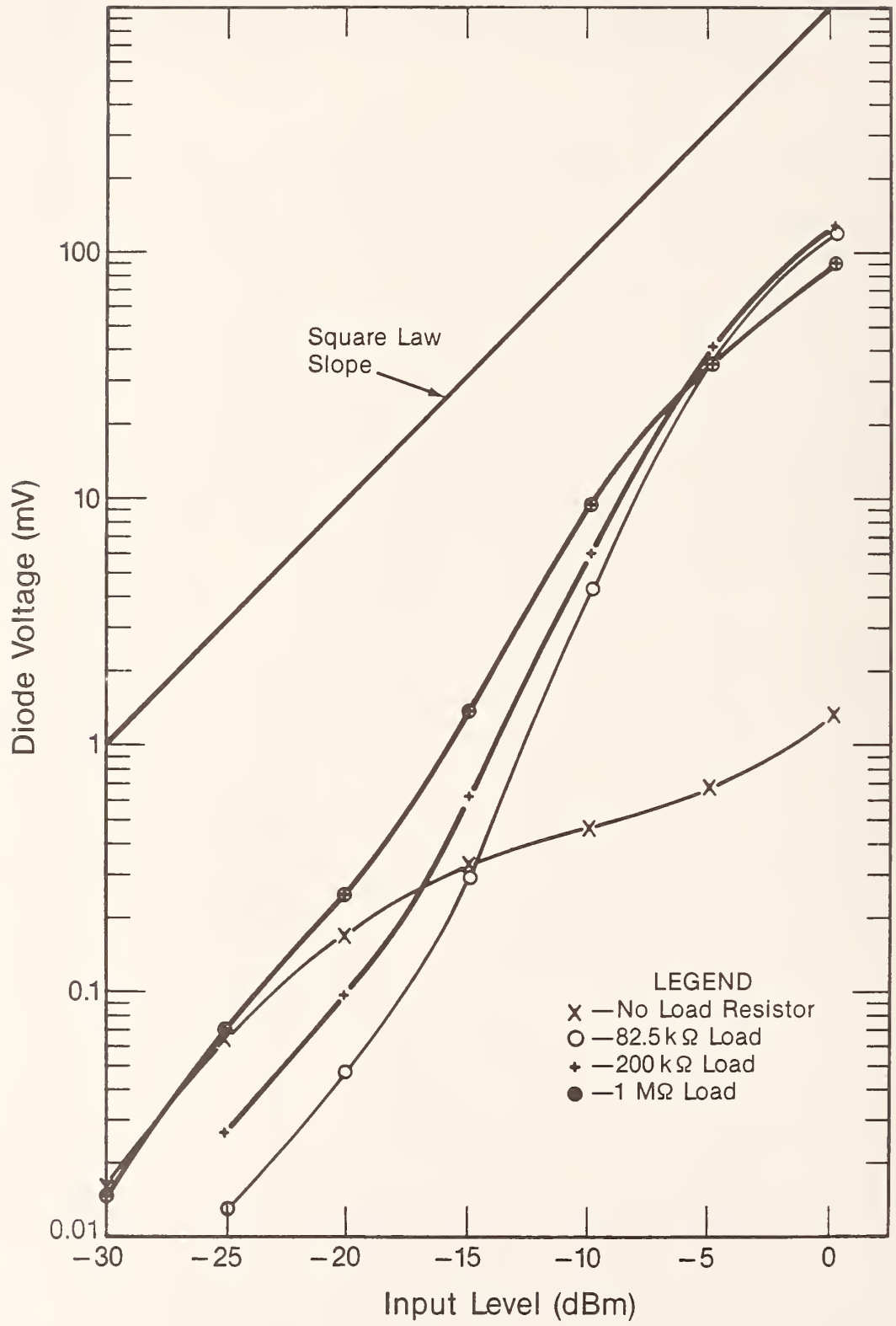

Figure 6. Finline diode detector response using different values of load resistors.

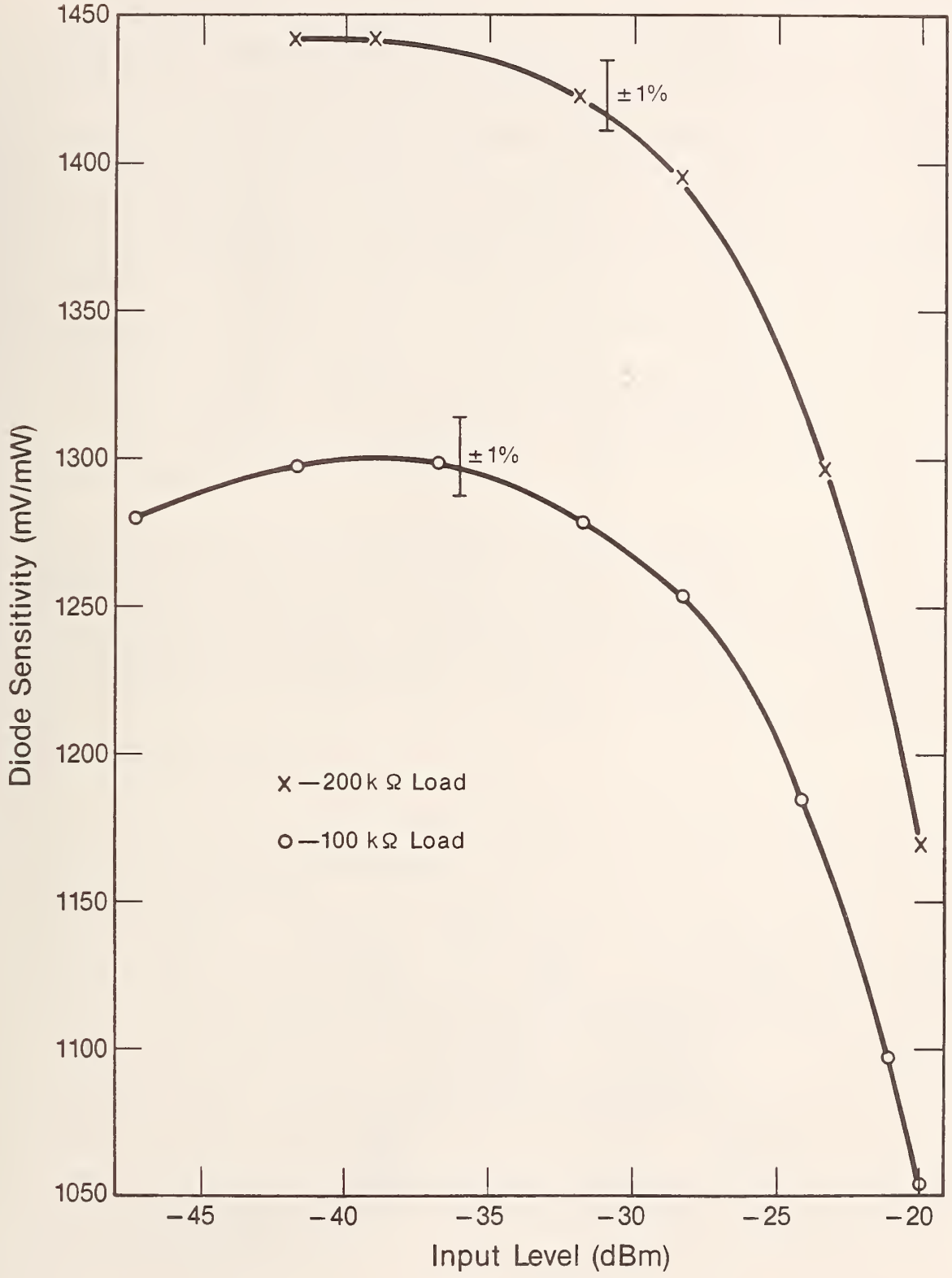

Figure 7. Finline diode detector response with expanded vertical scale.

3.3 Series slot tests

A second substrate was metalized with two different circuits, each having three slots, as shown in figure 8. One circuit had a finline gap of 0.762 mm and the other 0.381 mm. These circuits were built to test the three nondirectional probes which make up the correlator or phase information part of the six-port. The longitudinal spacing of the three slots was the estimated $\lambda_g/6$. The width of the three slots was 0.762 mm. Beam lead diodes were ultrasonically bonded across each of the slots. This places three impedances (diode impedance) in series with the finline and with $\lambda_g/6$ spacing along the finline. The nondirectional voltage coupling to each diode will be the ratio of the real part of its impedance to the impedance of the finline. If the coupling is weak (approximately 10 dB), each diode will detect approximately the same level.

Measurements on the series slot arrangement showed coupling to be relatively close to that estimated by typical models for the Schottky diode impedance and the previously estimated finline impedance. For the 0.762 mm finline, the impedance is approximately 200 ohms. The real part of the diode impedance should be around 20 to 30 ohms.

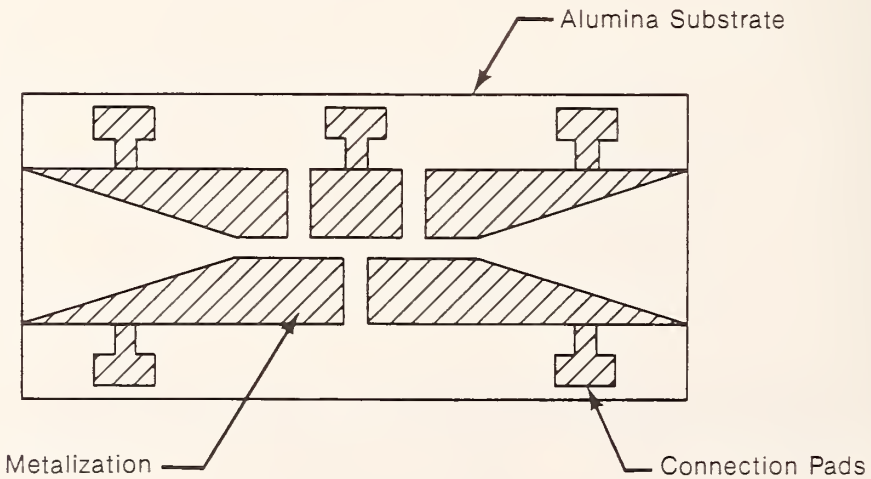

Figure 8. Series slot finline metalization.

Phase measurements were done by looking at the output from each diode, sliding a short at the output port of the finline circuit, and noting the position of the short (micrometer readout) for a null at each diode. Converting from distance to phase is a simple matter of knowing the guide wavelength in the rectangular waveguide, since the sliding short was mounted in WR-42 waveguide. The phase relationships between diodes were not anywhere near the 120° electrical spacing predicted. The probable cause of the problem in the phase measurements is multiple high reflections within the network.

4. Redesign

At this point in the work several things became apparent.

a) The leakage/loss problem had to solved.

b) The waveguide housing needed to be redesigned.

c) Multiple reflections within the WFW transition were masking effects which needed to be measured.

4.1 Leakage correction

Several of the finline papers [14-16] suggested putting serrations or transverse slots along the metalization where it passes through the broad wall in the rectangular waveguide, as shown in figure 9. This is done to suppress TEM propagation in the waveguide wall region. This technique is based on an old idea for probing fields in rectangular waveguide without disturbing the fields inside the guide [17]. This technique was tried on the next finline circuit, but an important point was missed. The metalized serrations should not extend beyond the outside of the waveguide wall. The serrations are merely open-circuited, quarter-wave transmission lines, sandwiched in the slot in the waveguide wall. If they protrude beyond the wall, they act like antennas, coupling energy out of the waveguide. Future fabrication will correct this problem.

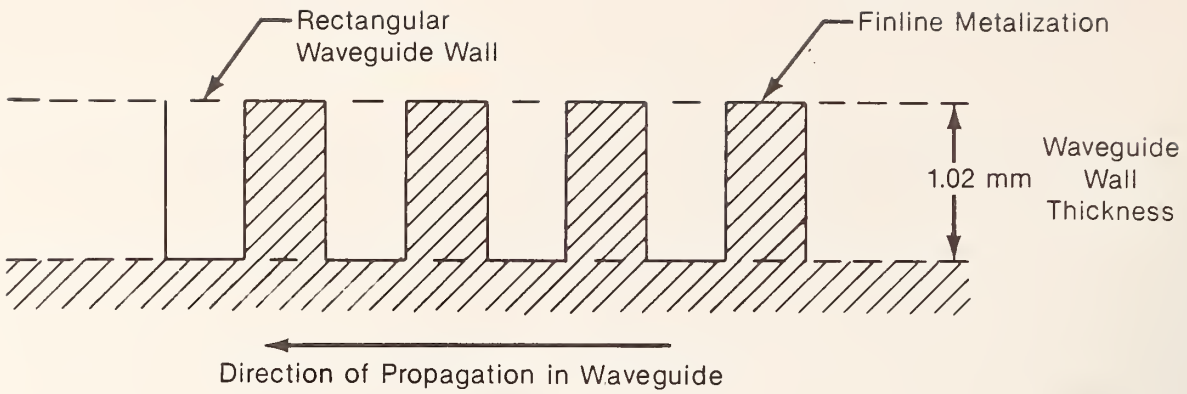

Figure 9. Serrations in finline metalization in waveguide wall region.

4.2 Waveguide housing

The waveguide housing was redesigned to more accurately and consistently locate the finline substrate within the waveguide. The new housing consists of two waveguide halves split down the center of the broad waveguide walls. Two slots the same length and width of the substrate are milled into one of the halves. The two halves are held together by screws which go through thick plates which form the narrow walls of the waveguide, as shown in figure 10.

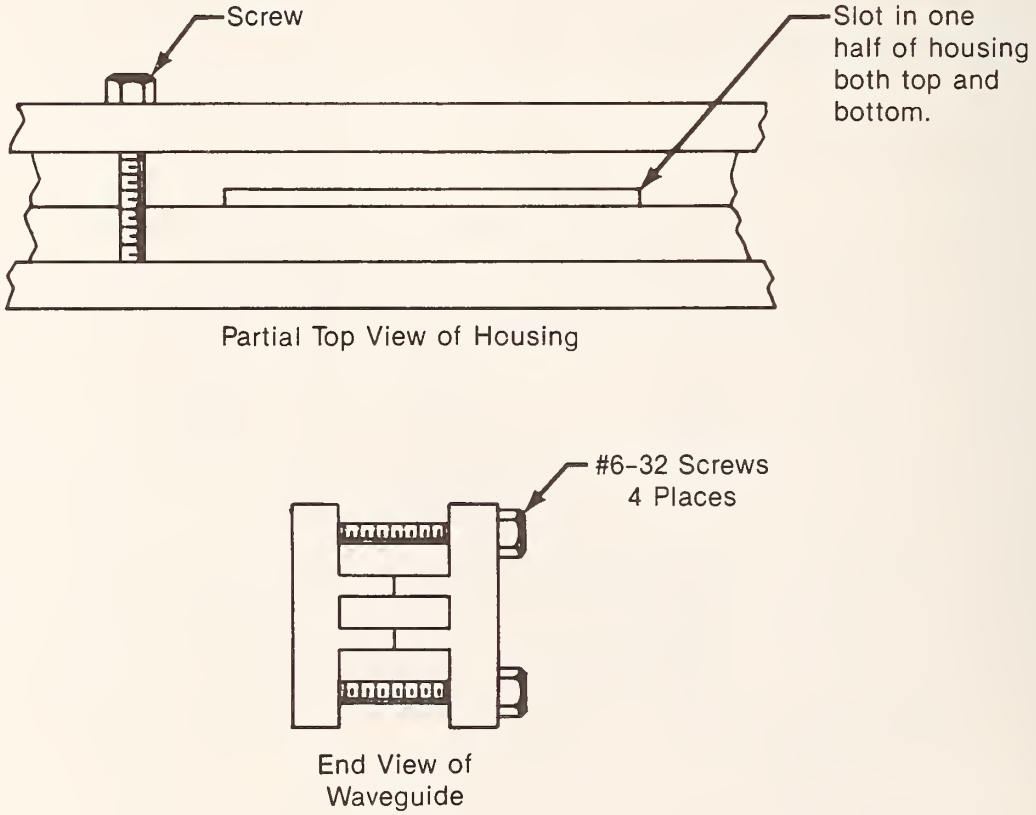

Figure 10. Waveguide housing for finline substrate.

4.3 Taper design

High reflections in the first two finline circuits led to a very intensive study of the propagation characteristics (λ_g, Z) for finline on alumina substrate. This resulted in two taper designs. The tapers are used for impedance matching at transmission line discontinuities. The two tapers are 1) for open waveguide to alumina slab loaded waveguide, and 2) for slab loaded waveguide to narrow gap finline.

4.3.1 Dielectric taper

Waves propagating down the open rectangular waveguide first encounter a discontinuity at the alumina substrate in the WFW transition. The high dielectric constant of the alumina, even in a very thin slab, concentrates the fields in the center of the guide and has the same effect on propagation that ridges or finline have. This effect lowers the cutoff frequency (f_c) and, as a result, increases the bandwidth of the waveguide. The slab also lowers the impedance of the waveguide, thus creating a high reflection. In order to study this problem, the transverse resonance method was used [18]. Consideration of a slab, parallel to the E field, centered in the waveguide leads to the transcendental equation,

$$\frac{Z_{01}}{Z_{02}} \tan \frac{\pi}{\lambda_{c_1}} (a-s) = \cot \frac{\pi}{\lambda_{c_2}} s, \tag{7}$$

where Z_{01} and Z_{02} are the respective impedances in the open and dielectric portions of the transverse section of waveguide; λ_{c1} and λ_{c2} the cutoff wavelengths in the open and dielectric sections; a, the waveguide width; and s, the dielectric slab thickness. λ_g can be obtained by using the relationship

$$\frac{Z_{01}}{Z_{02}} = \frac{\lambda_{c_1}}{\lambda_{c_2}} = \sqrt{\frac{\varepsilon_R - \left(\frac{\lambda_0}{\lambda_g}\right)^2}{1 - \left(\frac{\lambda_0}{\lambda_g}\right)^2}} \tag{8}$$

along with eq (7). The quantity ε_R is the slab relative dielectric constant and λ_0 the free space wavelength. The Newton-Rapheson technique was used with a computer to solve eqs (7) and (8) for λ_0/λ_g and λ_{cd} (cutoff wavelength of slab loaded waveguide). Figure 11 shows the effect of different dielectric

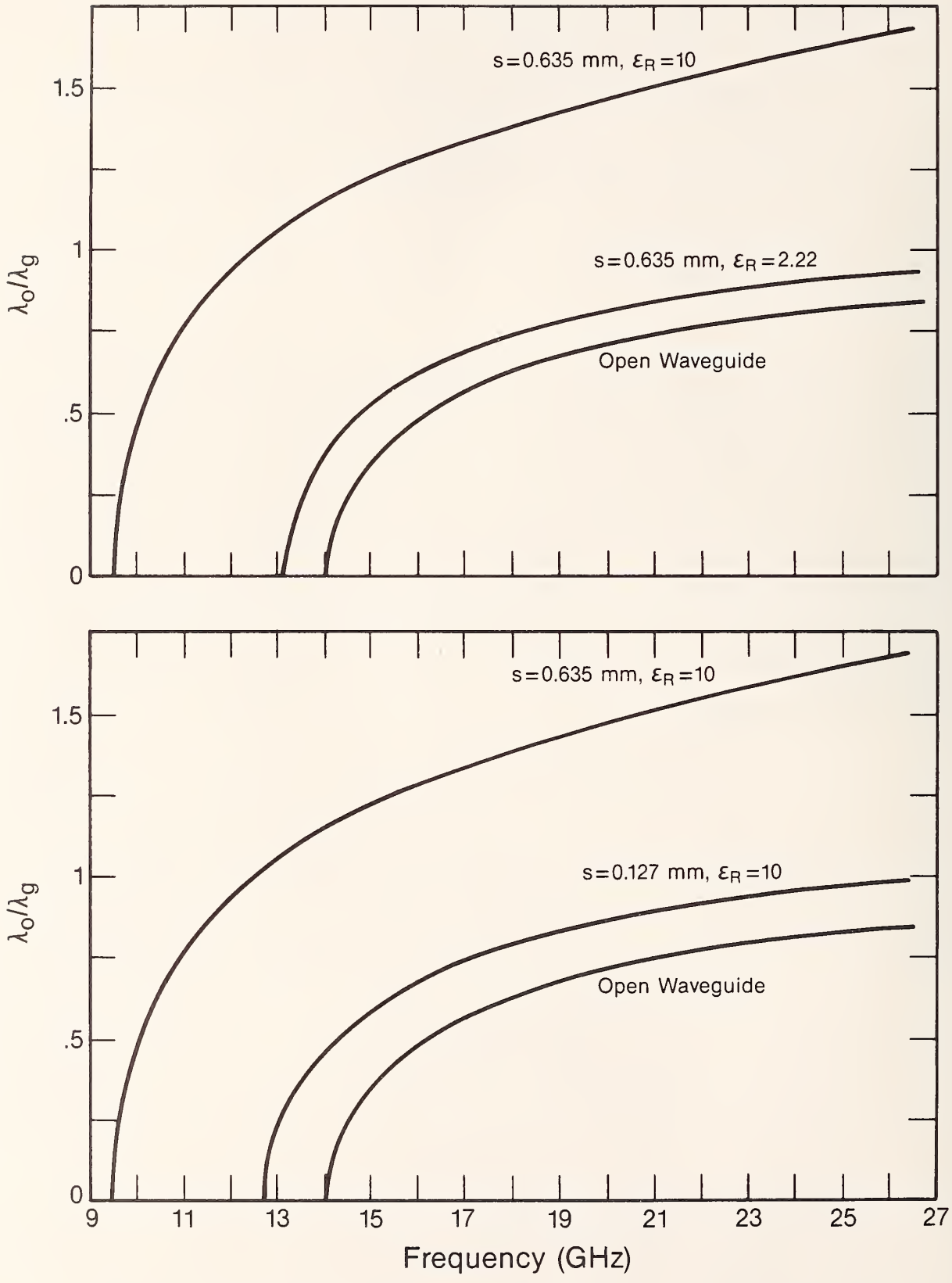

Figure 11. Guide wavelength and cutoff frequency effects for different slab loaded waveguides.

slabs on the guide wavelength and cutoff frequency (intersection with frequency axis). One additional complication arises when λ_0/λ_g is greater than unity, because eq (8) becomes complex and the use of hyperbolic functions in eq (7) is necessary. The computer program written to solve eqs (7) and (8) is versatile enough to handle a variety of slab loaded waveguide problems.

Once λ_g and λ_{cd} have been determined, the taper problem can be solved. The technique used is a numerical one, and is based on the first part of a paper by Johnson [19]. The assumptions are that multiple reflections and excitation of higher order modes are ignored. The taper is broken up into N sections and the reflection coefficient looking into the taper is (see fig. 12)

$$\Gamma \approx \sum_{n=1}^{N} \Gamma_n \exp\left[-2 \sum_{m=0}^{n-1} \gamma_m \Delta x\right] \tag{9}$$

where

$$\Gamma_n = \frac{Z_n - Z_{n-1}}{Z_n + Z_{n-1}}. \tag{10}$$

γ_m is the propagation constant of the mth section ($\gamma_m = \alpha_m + j\beta_m$) and assuming losslessness ($\alpha_m = 0$),

$$\gamma_m = j \frac{2\pi}{\lambda_{gm}}, \tag{11}$$

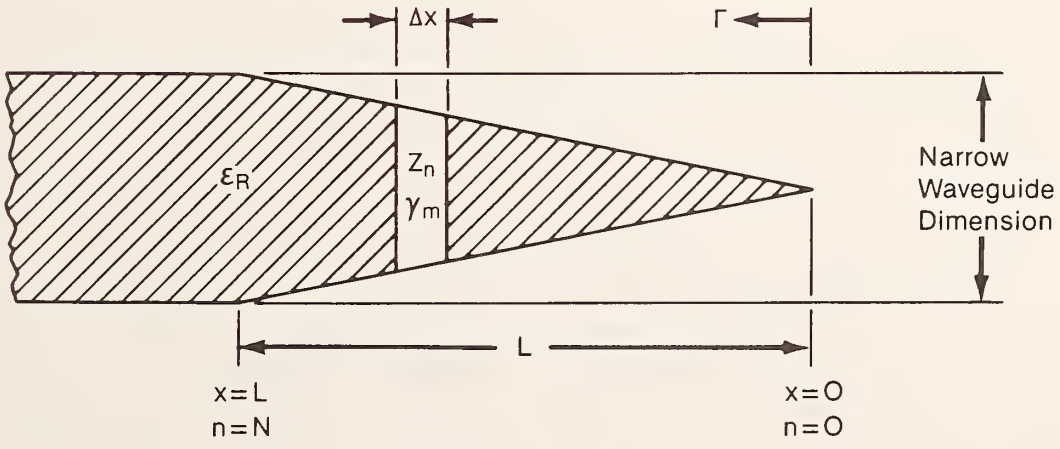

Figure 12. Physical representation for numerical solution of dielectric taper.

where λ_{gm} is obtained from eqs (7) and (8). Δx is L/N where L is the length of the taper. The impedances in eq (10) were calculated using the wave impedance definition

$$Z = \frac{\eta_0}{\sqrt{k_e - \left(\frac{c}{f}\right)^2}}, \tag{12}$$

where f_c is the cutoff frequency for an open waveguide and f is the frequency of interest. The parameter k_e varies from 1 in the open waveguide to a final value

$$k_e = \left(\frac{\lambda_0}{\lambda_g}\right)^2 + \left(\frac{f_c}{f}\right)^2, \tag{13}$$

where λ_g is the guide wavelength for the fully loaded guide. The intrinsic impedance, η_0, is the impedance at infinite frequency for an open waveguide (η_0 =377 ohms). For a linear taper, the assumption was made that k_e in eq (12) varies linearly from 1 to a value (k_e calculated using eq (13)), as x varies from 0 to L. In the case of an 0.635 mm alumina substrate, k_e = 2.524. Equations (7) through (12) were incorporated into a computer program to solve for taper reflection coefficient, Γ, for variable taper lengths, functional shape, and frequency. Figure 13 shows the results of this analysis. A linear taper (pointed triangle cut from alumina) 2.54 cm long was added to each end of the WFW transition, and the improvement in reflection agreed with the analysis.

The analytical approach, later in the Johnson paper [19], was also used to analyze different tapers. This involved considerable analytical work along with numerical approximations, and yielded similar but less accurate results. Figures 14 and 15 show results from this analysis. This approach takes the limit in eq (9) as $\Delta x \to 0$, which then leads to an integral equation for Γ (eq (14)). Integrating by parts leads to an expression for Γ containing three parts (eq (15)), the third of which is a difficult expression to evaluate. The third term is usually negligible. The name, two-term analysis, comes from the fact that the third term in eq (15) for Γ is negligible (for longer taper lengths).

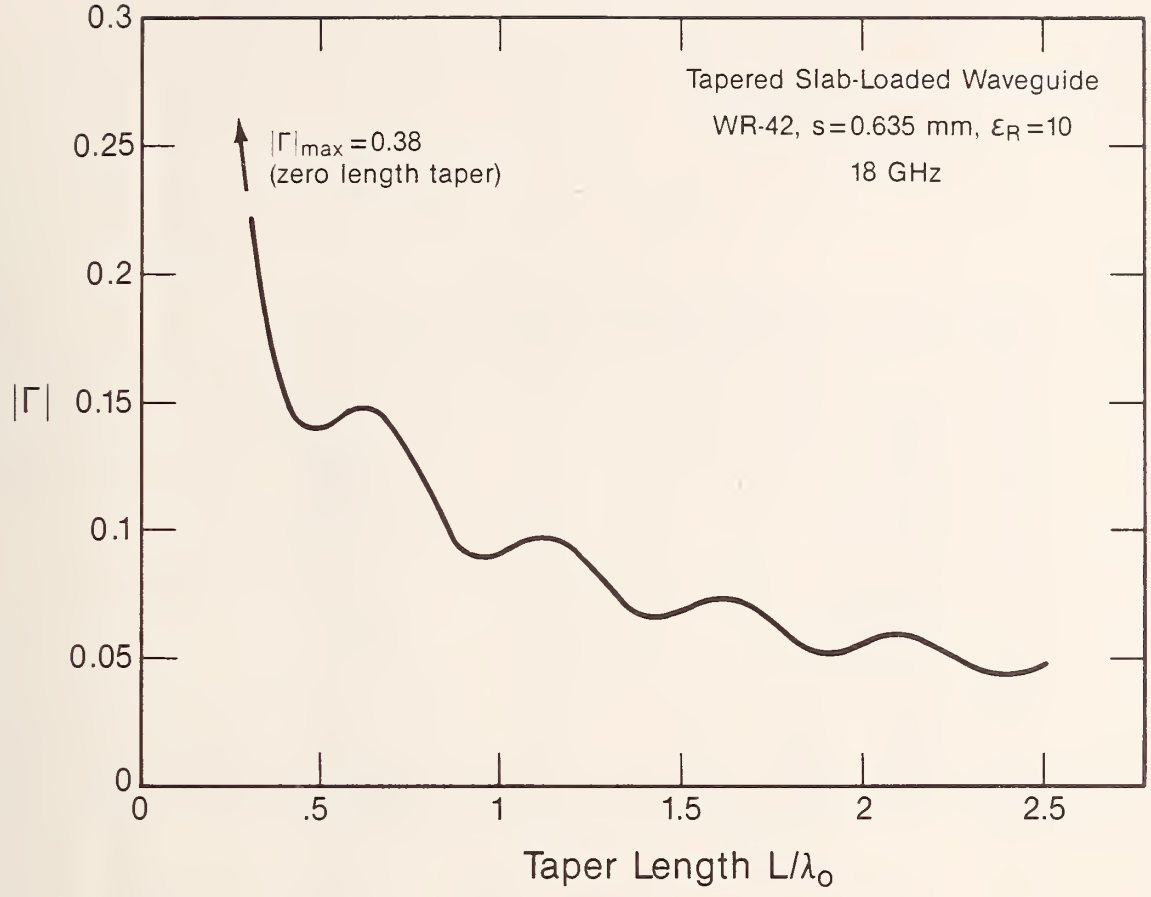

Figure 13. Numerical solution for reflection coefficient magnitude ($|\Gamma|$) for a linear dielectric taper.

$$\Gamma = \int_0^L \frac{1}{2} \left(\frac{d}{dx} \ln Z\right) \exp\left[-2 \int_0^x \gamma d\tau\right] dx, \tag{14}$$

and

$$\Gamma = \frac{1}{4\gamma_0} \left(\frac{d}{dx} \ln Z\right)_0 - \frac{1}{4\gamma_1} \left(\frac{d}{dx} \ln Z\right)_1 \exp\left[-2 \int_0^L \gamma dx\right] \tag{15}$$

$$+ \int_0^L \frac{d}{dx} \left(\frac{1}{4\gamma} \frac{d}{dx} \ln Z\right) \exp\left[-2 \int_0^x \gamma d\tau\right] dx.$$

The subscripts 0 and 1 refer to evaluation of the expression at x = 0 and x = L, and γ is the propagation constant ($\alpha + j\beta$), which in general is a function of x.

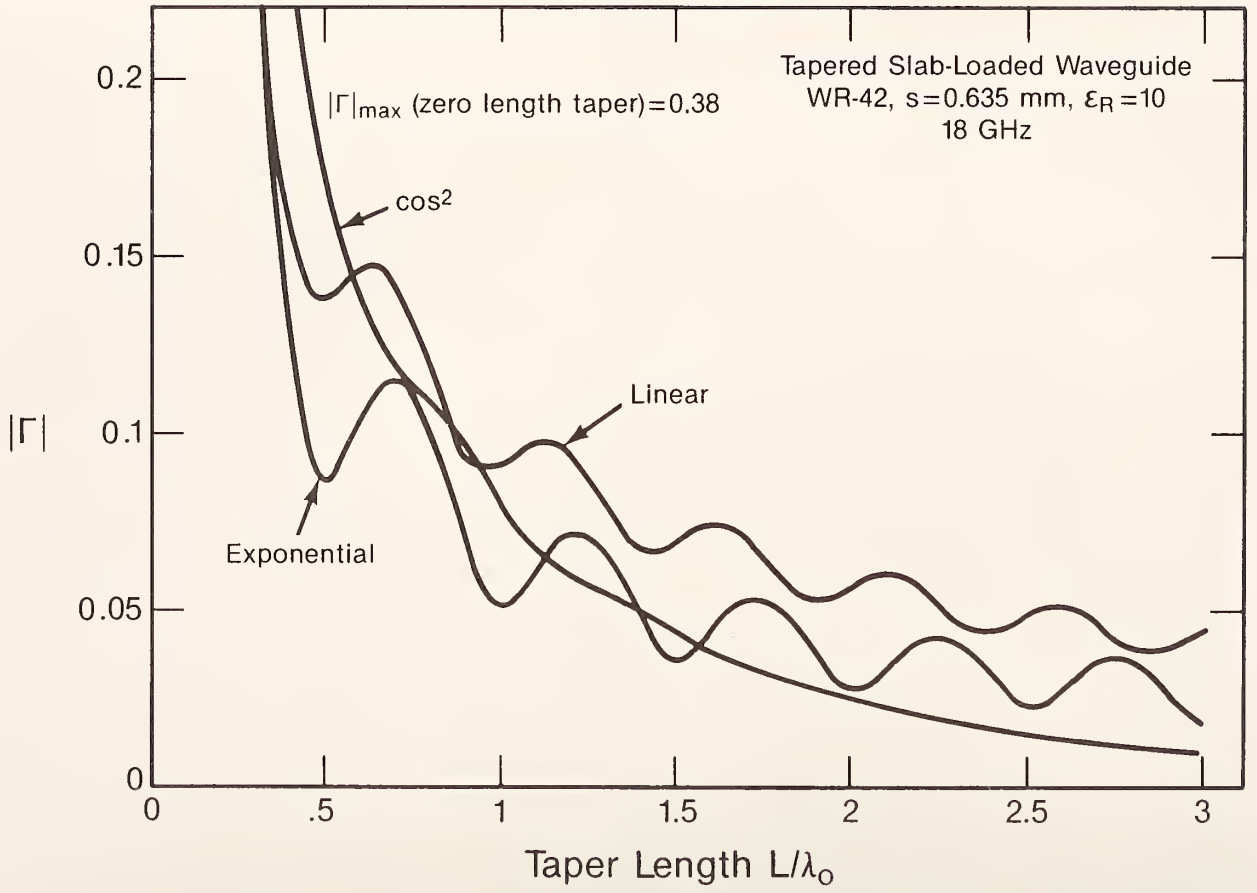

Figure 14. Two-term analysis for reflection coefficient magnitude ($|\Gamma|$) for various functional shapes of dielectric tapers at a fixed frequency.

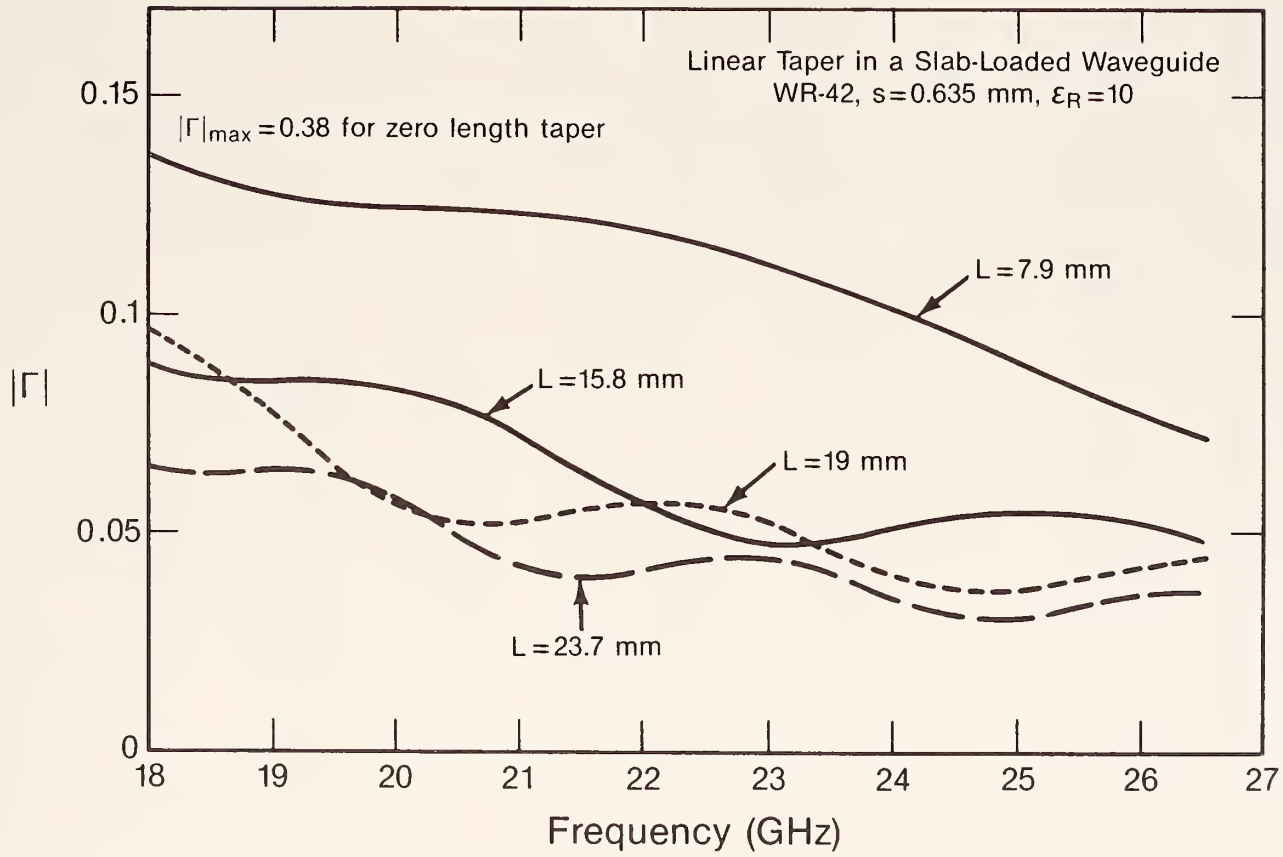

Figure 15. Two-term analysis for reflection coefficient magnitude ($|\Gamma|$) for various lengths of linear dielectric tapers across the WR-42 waveguide band.

4.3.2 Finline taper design

The finline propagation characteristics and taper analysis follow the same general ideas as the dielectric taper. There is the added complication of fins or ridges superimposed on a slab loaded waveguide. In the case of finline, it is necessary to solve three transcendental equations before obtaining λ_g and k_e. The physical dimensions occuring in the following equations are shown in figure 3. A transverse resonance solution is described in [20] and [21]. The sequence of solution for λ_g starts with an approximate, closed-form equation (16) for k_{ca} which is the cutoff wave number for air filled finline [22]. k_{ca} can also be solved for with a transcendental equation from [20].

$$k_{ca} = \frac{2\pi}{\lambda_{ca}} = \frac{\pi}{a}\left[1 + \frac{4}{\pi}\left(1 + 0.2\sqrt{\frac{b}{a}}\right)\frac{b}{a}\,\ell n\,\csc\left(\frac{\pi}{2}\frac{d}{b}\right)\right]^{-1/2}. \tag{16}$$

λ_{ca} is the cutoff wavelength of air filled finline (no substrate). The next step is to solve eq (17) for k_{cd}, the cutoff wave number for dielectric filled finline [20].

$$-\cot\left(\frac{a\,k_{cd}}{2}\right) - \cot\left[k_{cd}\left(\frac{a}{2} - s\right)\right] + \frac{B_u}{Y_b} = 0. \tag{17}$$

In eq (17),

$$\frac{B_u}{Y_b} = \frac{b}{\pi}\,k_{cd}\left[P_w + \varepsilon_R(P_d + P_b)\right] \tag{18}$$

where

$$P_w = \ell n\left[\csc\left(\frac{\pi d}{2b}\right)\right], \tag{19}$$

$$P_d = \frac{s}{d}\arctan\left(\frac{d}{s}\right) + \ell n\sqrt{1 + \left(\frac{s}{d}\right)^2}, \tag{20}$$

and

$$P_b = \frac{s}{b}\arctan\left(\frac{b}{s}\right) + \ell n\sqrt{1 + \left(\frac{s}{b}\right)^2}. \tag{21}$$

Then, with k_{cd} from eqs (17)-(21) and k_{ca} from eq (16), the constant k_c can be solved using eq (22)

$$k_c = \left(\frac{k_{ca}}{k_{cd}}\right)^2. \tag{22}$$

The constant k_c is the equivalent dielectric constant at cutoff. The parameter k_e ([2]) is the equivalent dielectric constant, which in general is a function of frequency. k_e is used to calculate guide wavelength, λ_g, using eq (23)

$$\frac{\lambda_g}{\lambda_o} = \sqrt{k_e - \left(\frac{k_{ca}}{k_o}\right)^2}, \tag{23}$$

where k_o is $\frac{2\pi}{\lambda_o}$. If the dielectric is very thin $\left(\frac{s}{b} << 1\right)$, and/or the dielectric constant is low ($\varepsilon_R \approx 1$), then k_e is not a function of frequency and is approximately k_c. No more computation is necessary in this case to determine λ_g. If, however, alumina substrates are used, more computation is necessary. After determining k_c, eqs (24)-(26) are used to get λ_g [21]. Solve for $\bar{x}$ in eq (24)

$$\cot\left(\frac{\pi}{2}\,\bar{x}\,\sqrt{\frac{\varepsilon_R}{k_c}}\right) - \sqrt{\varepsilon_R}\,\tan\left[\frac{\pi}{2}\,(1-\bar{x})\,\sqrt{\frac{1}{k_c}}\,\right] = 0. \tag{24}$$

Then solve for $\varepsilon_e(f)$ in eq (25)

$$\cot\left(\frac{\pi}{2}\,\bar{x}\,\frac{\lambda_{ca}}{\lambda_o}\,\sqrt{\varepsilon_R}\right) - \sqrt{\frac{\varepsilon_R - \varepsilon_e}{1-\varepsilon_e}}\,\tan\left[\frac{\pi}{2}\,(1-\bar{x})\,\frac{\lambda_{ca}}{\lambda_o}\,\sqrt{1-\varepsilon_o}\right] = 0 \tag{25}$$

where $\frac{\lambda_{ca}}{\lambda_o} = \frac{k_o}{k_{ca}}$ from eq (16) and $k_o = \frac{2\pi}{\lambda_o}$. Equation (26) shows the relationship between ε_e, k_e, and λ_g

$$\varepsilon_e(f) = \left(\frac{\lambda_o}{\lambda_g}\right)^2 = k_e(f) - \left(\frac{\lambda_o}{\lambda_{ca}}\right)^2. \tag{26}$$

The process from eqs (16)-(26) has been computerized to obtain λ_g as a function of waveguide dimensions -a and b, gap width -d, substrate thickness -s, dielectric constant -ε_R, and frequency.

In order to completely characterize finline, an impedance needs to be defined and calculated. One definition and method of solution is given in [22]. This definition is a voltage-current definition, but as long as the same definition is used throughout an analysis (for example, throughout a taper in a taper analysis), the results should be accurate. The impedance (Z_o) from [22], is

$$Z_0 = \frac{Z_{0_\infty}}{\sqrt{k_e - \left(\frac{\lambda_0}{\lambda_{ca}}\right)^2}} \tag{27}$$

where k_e and $\frac{\lambda_0}{\lambda_{ca}}$ have already been calculated, and Z_{0_∞} is the impedance at infinite frequency from eqs (28)-(31).

$$Z_{0_\infty} = \frac{120\ \pi^2\ \left(\frac{b}{\lambda_{ca}}\right)}{\frac{b}{d} \sin \frac{\pi s}{\lambda_{ca}} \left[\frac{B_0}{Y_0} + \tan \frac{\pi}{2} \frac{(a - s)}{\lambda_{ca}}\right] \cos \frac{\pi s}{\lambda_{ca}}}, \tag{28}$$

where

$$\frac{B_0}{Y_0} = \frac{2b}{\lambda_{ca}} \left[\ln \csc \alpha + \frac{Q\cos^4\alpha}{1+Q\sin^4\alpha} + 16 \left(\frac{b}{\lambda_{ca}}\right)^2 \left(1 - 3\sin^2\alpha\right)^2 \cos^4\alpha\right] \tag{29}$$

$$\alpha = \frac{\pi}{2} \frac{d}{b} \tag{30}$$

and

$$Q = \left[1 - \left(\frac{b}{\lambda_{ca}}\right)^2\right]^{-1/2} - 1. \tag{31}$$

A simpler approximation for $\frac{B_0}{Y_0}$ is

$$\frac{B_0}{Y_0} = \frac{2b}{\lambda_{ca}} \ln \csc \alpha. \tag{32}$$

At this stage, a taper can be analyzed by using either the two-term or numerical technique described in the preceding section. After programing the λ_g and Z_0 solutions and doing a two-term analysis, figures 16 and 17 show the results for various finline tapers on alumina substrate, plotted using a computer.

An exponential finline taper, along with a linear dielectric taper, was fabricated for a waveguide-finline-waveguide transition and a series slot configuration. The serrations were also included, although they protruded from the waveguide. Measurements showed that the reflection problems were solved, but the high loss was still there. The loss can be removed as described in 4.1. The reflection coefficient of the WFW transition was less than 0.2 across the band ($|\Gamma| < 0.1$ over most of the band). The WFW

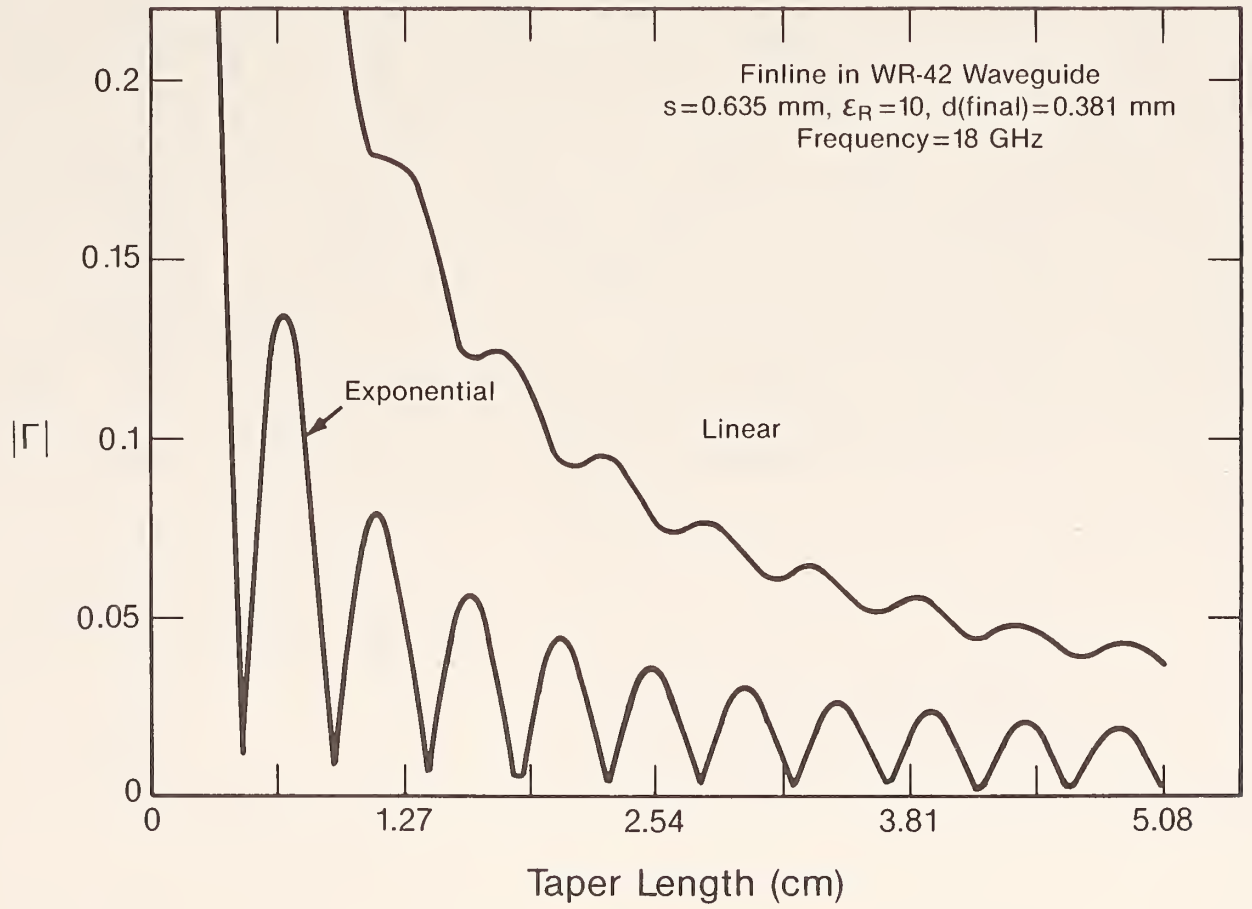

Figure 16. Reflection coefficient magnitude for exponential and linear tapers vs. taper length at 18 GHz.

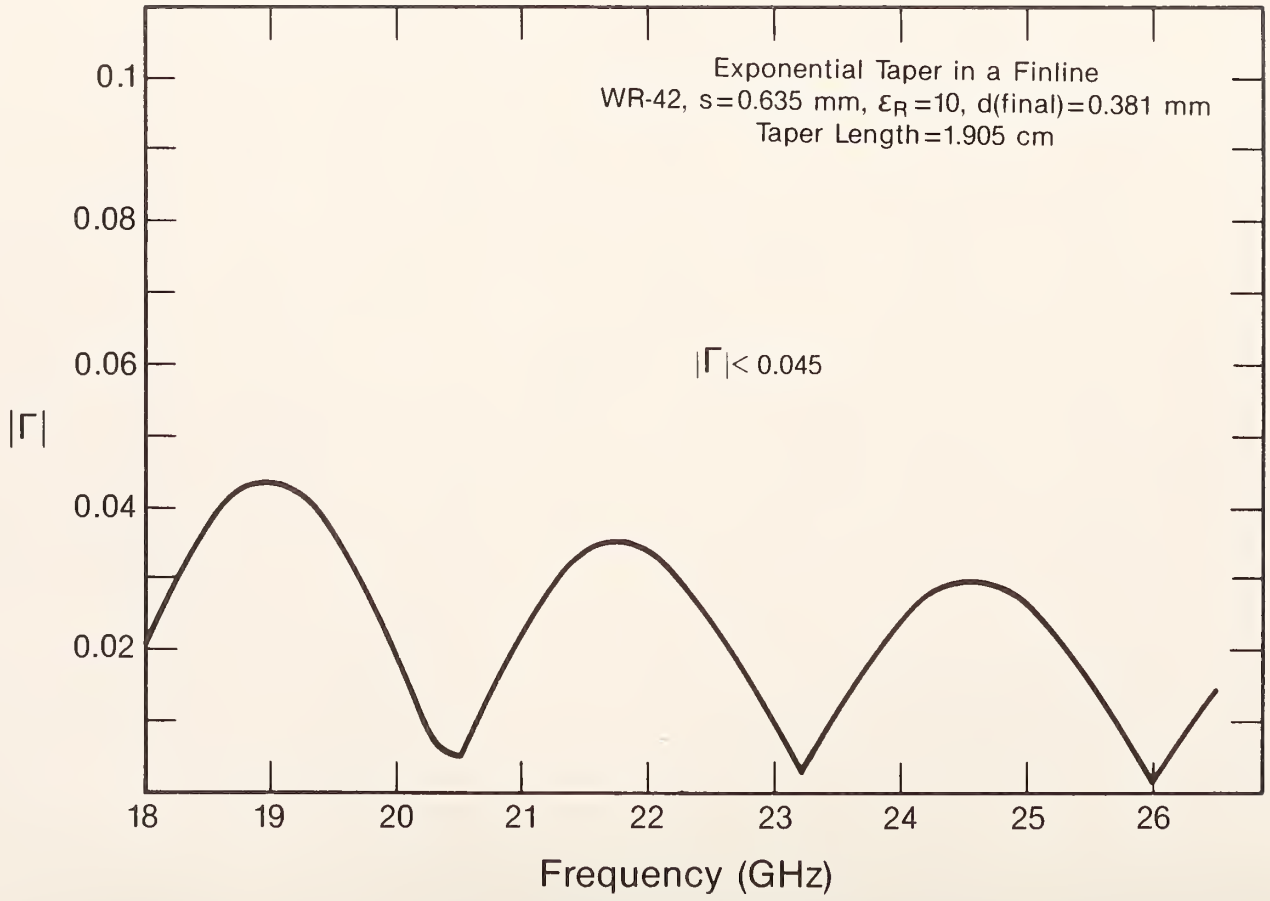

Figure 17. Reflection coefficient magnitude vs. frequency for exponential finline taper.

transition has four discontinuities or tapers, and the results agree well with the analyses in 4.3.1 and 4.3.2.

The internally terminated WFW transition measured $|S_{11}| < 0.07$ with loss > 25 dB. The internal load removes two tapers from the measurement leaving the result from one dielectric taper and one finline taper. The > 25 dB loss is an improvement over initial designs and will be improved more by trimming the metalization outside the waveguide.

4.3.3 Soft substrate designs

An alternate approach to using alumina as a substrate would be to use teflon-fiberglass ($\varepsilon_R = 2.22$). One reason for using teflon-fiberglass is that fabrication (using commercially available, metalized substrates)is easier. The lower dielectric constant of teflon-fiberglass also simplifies the analysis of the propagation characteristics of the finline and reduces the effects of the high dielectric constant of alumina. The diodes would have to be attached after fabrication of the finline circuit. A design analysis was done for teflon-fiberglass substrate in order to come up with a prototype six-port sooner than the work with alumina would allow. No hardware was fabricated, but a description of the analysis is included here for possible use in future work. Recently available, empirical equations for λ_g and Z_o were used to analyze the soft substrate finline [23].

Another recent paper [24] describes a geometric taper design for finline. This design involves two tangential circles to form the functional shape of the taper. It is a simple geometric design, and a pattern for finline on teflon-fiberglass was drawn using a computer graphics package. This design has not yet been implemented. Figure 18 shows the geometry of the two-circle taper, and figure 19 shows the results of a numerical analysis of the reflection coefficient of this taper compared to a linear and exponential taper (teflon-fiberglass substrate). The object of the design is to make the point of tangency of the two circles such that the impedance at L/2 (half the taper length) is equal to the average of the impedance at either end of the taper. The impedance calculations were done using the closed form equations [23]. This calculation then gives the gap width at L/2 or P_m in figure 18. The impedance does not follow the same curve as the physical dimensions, so the

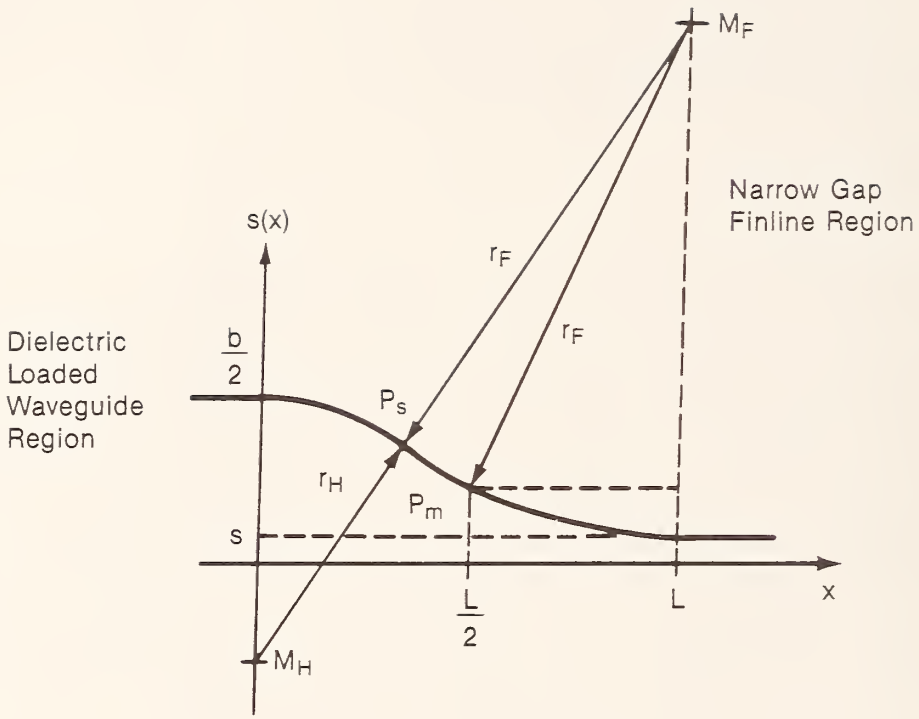

s(x) = taper shape (finline gap spacing)
M_H = center of first circle
r_H = radius of first circle
M_F = center of final circle
r_F = radius of final circle
P_s = point of tangency
P_m = point where $z = \frac{Z_{in} + z_{out}}{2}$
s = final finline gap width

Figure 18. Two-circle taper showing the geometry of one-half of the taper (full taper would include mirror image of curve shown).

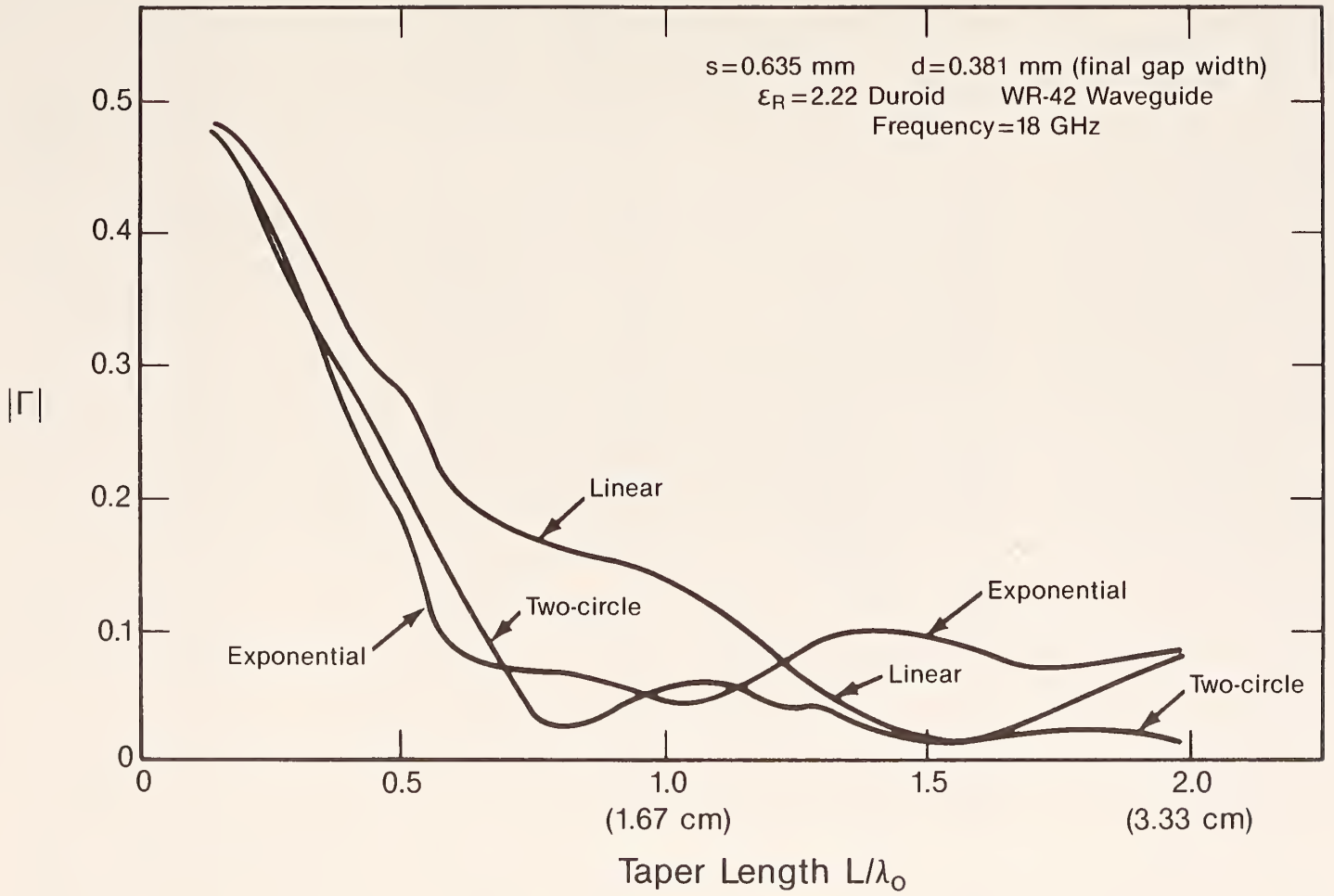

Figure 19. Reflection coefficient for three functional shapes of finline tapers on Duroid substrate (finite numerical analysis).

tangency point tends to be toward the open end of the taper (radius r_F is much larger than radius r_H). The slope of the taper at either end is zero, so a two-term analysis would give a reflection coefficient of zero; the derivative $\frac{d}{dx}(\ell nZ)$ in eq (15), evaluated at either end would be zero. Figure 19, which comes from a numerical analysis, does not yield a zero reflection coefficient (the two-term analysis is only approximate). The two-circle taper appears to be as good or better than the exponential taper for matching. It is also easier to make a pattern for the two-circle taper than it is for the exponential taper.

5. Summary and future work

Initial designs of finline circuits which could lead to the fabrication of integrated diode six-ports for use above 18 GHz were unacceptable. High losses and reflections led to improved designs. A great deal of effort was put into analyzing slab loaded waveguide and finline. This effort led to the design of tapers for finline on alumina. Work was also done on the design of finline on teflon-fiberglass.

Future work should start with the fabrication and testing of finline on alumina with no protrusion of the metalization from the waveguide. If all goes well, a directional coupler can be built and tested, and finally a six-port with beam lead diodes in WR-42 waveguide built and tested. In the event that alumina still gives problems, a teflon-fiberglass substrate can be used to build a six-port. Ultimately an integrated diode six-port still has a good probability of realization.

6. Acknowledgment

The author wishes to thank R. Ginley for his work in fabricating the finline circuits and also members of the NBS Cryoelectronics Metrology Group for their suggestions and the use of their fabrication facility.

7. References

[1] Russell, D. H.; Weidman, M. P. Millimeter wave six-ports. Wiltse, J. C., ed. Proceedings of the International Society of Photoptical Engineering (SPIE); Vol. 544:162-168; 1985 April 9-10; Arlington, VA.

[2] Meier, P. J. Integrated fin-line millimeter components. IEEE Trans. Microwave Theory Tech. (U.S.) 22(12): 1209-1216; 1974 December.

[3] Solbach, K. The status of printed millimeter-wave printed E-plane circuits. IEEE Trans. Microwave Theory Tech. (U.S.) 31(2): 107-121; 1983 February.

[4] Gupta, K. C.; Garg, R.; Bahl, I.J. Slotlines I, chapter 5 in Microstrip lines and slotlines. Massachusetts: Artech House, Inc.; 1979. 197-223.

[5] Knorr, J. B.; Shayda, P. M. Millimeter-wave fin-line characteristics. IEEE Trans. Microwave Theory Tech. (U.S.) 28(7): 737-742; 1980 July.

[6] Gupta, K. C.; Garg, R.; Bahl, I.J. Slotlines I, chapter 8 in Microstrip lines and slotlines. Massachusetts: Artech House, Inc.; 1979. 303-313, 352-362.

[7] Knorr, J. B.; Kuchler, K. D. Analysis of coupled slots and coplanar strips on dielectric substrate. IEEE Trans. Microwave Theory Tech. (U.S.) 23(7): 541-548; 1975 July.

[8] Rudokas, R.; Itoh, T. Passive millimeter-wave IC components made of inverted strip dielectric waveguides. IEEE Trans. Microwave Theory Tech. (U.S.) 24(12): 978-981; 1976 December.

[9] Kpodzo, E.; Schunemann, K.; Begemann, G. A quadraphase fin-line modulator. IEEE Trans. Microwave Theory Tech. (U.S.) 28(7): 747-752; 1980 July.

[10] Sharma, A. K.; Hoefer, W. K. Propagation in coupled unilateral and bilateral finlines. IEEE Trans. Microwave Theory Tech. (U.S.) 31(6): 498-501; 1983 June.

[11] Mariana, E. A.; Agrios, J. P. Slot-line filters and couplers. IEEE Trans. Microwave Theory Tech. (U.S.) 18(12): 1089-1094; 1970 December.

[12] Levy, R. Directional couplers. Chapter 3, Advances in microwaves, Vol. 1. L. Young, ed. New York: academic Press; 1966. 115-209.

[13] Engen, G. F. Theory of UHF and microwave measurements using the power equation concept. Nat. Bur. Stand. (U.S.) Tech. Note 637; 1973 April. 63 p.

[14] Meier, P. J. Millimeter integrated circuits suspended in the E-plane of rectangular waveguide. IEEE Trans. Microwave Theory Tech. (U.S.) 26(10):726-733; 1978 October.

[15] Meier, P. J. New developments with integrated fin-line and related printed millimeter circuits. IEEE MTT-S International Symposium Digest (U.S.). 143-145; 1975 May 12-14; Palo Alto, CA.

[16] VanHeuven, J. H. C. A new integrated waveguide-microstrip transition. IEEE Trans. Microwave Theory Tech. (U.S.) 24(3):144-147; 1976 March.

[17] Tomiyasu, K.; Bolus, J. J. Characteristics of a new serrated choke. IRE Trans. Microwave Theory Tech. (U.S.) 4(1): 33-36; 1956 January.

[18] Marcuvitz, N. Propagation in composite guides. Chapter 8.1 in Waveguide handbook, Vol. 10 of Rad. Lab. Series. N. Marcuvitz, ed. New York: McGraw Hill Book Co., Inc.; 1951. 388-391.

[19] Johnson, R. C. Design of linear double tapers in rectangular waveguides. IRE Trans. Microwave Theory Tech. (U.S.) 7(3): 374-378; 1959 July.

[20] Piotrowski, J. K. Accurate and simple formulas for dispersion in finlines. IEEE MTT-S International Symposium Digest (U.S.) 333-335; 1984 May 30-June 1; San Francisco, CA.

[21] Pramanick, P.; Bhartia, P. Analysis and synthesis of tapered finlines. IEEE MTT-S International Symposium Digest (U.S.) 336-338; 1984 May 30-June 1; San Francisco, CA.

[22] Hoefer, W.J.R.; Burton, M. N. Closed form expressions for the parameters of finned and ridged waveguides. IEEE Trans. Microwave Theory Tech. (U.S.) 30(12): 2190-2194; 1982 December.

[23] Pramanick, P.; Bhartia, P. Accurate analysis equations and synthesis technique for unilateral finline. IEEE Trans. Microwave Theory Tech. (U.S.) 33(1): 24-30; 1985 January.

[24] Beyer, A.; Wolff, I. Finline taper design made easy. IEEE MTT-S International Symposium Digest (U.S.) 493-496; 1985 June 3-5; St. Louis, MO.

NBS-114A (REV. 2-8C)

U.S. DEPT. OF COMM. BIBLIOGRAPHIC DATA SHEET (See instructions)	1. PUBLICATION OR REPORT NO. NBS TN-1090	2. Performing Organ. Report No.	3. Publication Date December 1985

4. TITLE AND SUBTITLE

Finline Diode Six-Port: Fundamentals and Design Information

5. AUTHOR(S)

M. Weidman

6. PERFORMING ORGANIZATION (If joint or other than NBS, see instructions)

NATIONAL BUREAU OF STANDARDS
DEPARTMENT OF COMMERCE
WASHINGTON, D.C. 20234

7. Contract/Grant No.

8. Type of Report & Period Covered

9. SPONSORING ORGANIZATION NAME AND COMPLETE ADDRESS (Street, City, State, ZIP)

10. SUPPLEMENTARY NOTES

☐ Document describes a computer program; SF-185, FIPS Software Summary, is attached.

11. ABSTRACT (A 200-word or less factual summary of most significant information. If document includes a significant bibliography or literature survey, mention it here)

The preliminary design and testing of a planar circuit six-port with diode detectors is described. The planar circuit medium was chosen to be finline, and all preliminary work was done in WR-42 waveguide (18-26.5 GHz). The finline substrate was alumina, and initially commercial beam-lead diodes were bonded to the finline metalization. The goal is to design an integrated circuit which could be fabricated on one chip (with diode detectors) and used as part of a six-port network analyzer in the waveguide bands above 18 GHz. Initial designs proved to be unsatisfactory because of high losses and reflections. Most of the problems have been solved, and a usable integrated finline circuit is a good possibility for a millimeter wave six-port.

12. KEY WORDS (Six to twelve entries; alphabetical order; capitalize only proper names; and separate key words by semicolons)

diode six-port; finline; integrated circuit; millimeter wave; network analyzer; planar circuit; six-port.

13. AVAILABILITY

☒ Unlimited

☐ For Official Distribution. Do Not Release to NTIS

☒ Order From Superintendent of Documents, U.S. Government Printing Office, Washington, D.C. 20402.

☐ Order From National Technical Information Service (NTIS), Springfield, VA. 22161

14. NO. OF PRINTED PAGES

40

15. Price

USCOMM-DC 6043-P80

☆ U.S. GOVERNMENT PRINTING OFFICE: 1985—677-285/45,082 REGION NO. 8

NBS Technical Publications

Periodical

Journal of Research—The Journal of Research of the National Bureau of Standards reports NBS research and development in those disciplines of the physical and engineering sciences in which the Bureau is active. These include physics, chemistry, engineering, mathematics, and computer sciences. Papers cover a broad range of subjects, with major emphasis on measurement methodology and the basic technology underlying standardization. Also included from time to time are survey articles on topics closely related to the Bureau's technical and scientific programs. Issued six times a year.

Nonperiodicals

Monographs—Major contributions to the technical literature on various subjects related to the Bureau's scientific and technical activities.

Handbooks—Recommended codes of engineering and industrial practice (including safety codes) developed in cooperation with interested industries, professional organizations, and regulatory bodies.

Special Publications—Include proceedings of conferences sponsored by NBS, NBS annual reports, and other special publications appropriate to this grouping such as wall charts, pocket cards, and bibliographies.

Applied Mathematics Series—Mathematical tables, manuals, and studies of special interest to physicists, engineers, chemists, biologists, mathematicians, computer programmers, and others engaged in scientific and technical work.

National Standard Reference Data Series—Provides quantitative data on the physical and chemical properties of materials, compiled from the world's literature and critically evaluated. Developed under a worldwide program coordinated by NBS under the authority of the National Standard Data Act (Public Law 90-396). NOTE: The Journal of Physical and Chemical Reference Data (JPCRD) is published quarterly for NBS by the American Chemical Society (ACS) and the American Institute of Physics (AIP). Subscriptions, reprints, and supplements are available from ACS, 1155 Sixteenth St., NW, Washington, DC 20056.

Building Science Series—Disseminates technical information developed at the Bureau on building materials, components, systems, and whole structures. The series presents research results, test methods, and performance criteria related to the structural and environmental functions and the durability and safety characteristics of building elements and systems.

Technical Notes—Studies or reports which are complete in themselves but restrictive in their treatment of a subject. Analogous to monographs but not so comprehensive in scope or definitive in treatment of the subject area. Often serve as a vehicle for final reports of work performed at NBS under the sponsorship of other government agencies.

Voluntary Product Standards—Developed under procedures published by the Department of Commerce in Part 10, Title 15, of the Code of Federal Regulations. The standards establish nationally recognized requirements for products, and provide all concerned interests with a basis for common understanding of the characteristics of the products. NBS administers this program as a supplement to the activities of the private sector standardizing organizations.

Consumer Information Series—Practical information, based on NBS research and experience, covering areas of interest to the consumer. Easily understandable language and illustrations provide useful background knowledge for shopping in today's technological marketplace.

Order the **above** *NBS publications from: Superintendent of Documents, Government Printing Office, Washington, DC 20402.*

Order the **following** *NBS publications—FIPS and NBSIR's—from the National Technical Information Service, Springfield, VA 22161.*

Federal Information Processing Standards Publications (FIPS PUB)—Publications in this series collectively constitute the Federal Information Processing Standards Register. The Register serves as the official source of information in the Federal Government regarding standards issued by NBS pursuant to the Federal Property and Administrative Services Act of 1949 as amended, Public Law 89-306 (79 Stat. 1127), and as implemented by Executive Order 11717 (38 FR 12315, dated May 11, 1973) and Part 6 of Title 15 CFR (Code of Federal Regulations).

NBS Interagency Reports (NBSIR)—A special series of interim or final reports on work performed by NBS for outside sponsors (both government and non-government). In general, initial distribution is handled by the sponsor; public distribution is by the National Technical Information Service, Springfield, VA 22161, in paper copy or microfiche form.

U.S. Department of Commerce
National Bureau of Standards
Gaithersburg, MD 20899

Official Business
Penalty for Private Use $300

POSTAGE AND FEES PAID
U S DEPARTMENT OF COMMERCE
COM-215

FIRST CLASS